Capabilities of 1D CUF-based models to analyse metallic/composite rotors

Matteo Filippi[*] and Erasmo Carrera

Department of Mechanical and Aerospace Engineering, Politecnico di Torino, Italy

Abstract.   The Carrera Unified Formulation (CUF) is here extended to perform free-vibrational analyses of rotating structures. CUF is a hierarchical formulation, which enables one to obtain refined structural theories by writing the unknown displacement variables using generic functions of the cross-section coordinates (x, z). In this work, Taylor-like expansions are used. The increase of the theory order leads to three-dimensional solutions while, the classical beam models can be obtained as particular cases of the linear theory. The Finite Element technique is used to solve the weak form of the three-dimensional differential equations of motion in terms of 'fundamental nuclei', whose forms do not depend on the adopted approximation. Including both gyroscopic and stiffening contributions, structures rotating about either transversal or longitudinal axis can be considered. In particular, the dynamic characteristics of thin-walled cylinders and composite blades are investigated to predict the frequency variations with the rotational speed. The results reveal that the present one-dimensional approach combines a significant accuracy with a very low computational cost compared with 2D and 3D solutions. The advantages are especially evident when deformable and composite structures are analyzed.

Keywords: composites; carrera unified formulation; finite element method; rotordynamics

1. Introduction

Many engineering applications require the use of rotating structures, whose design can represent a crucial task of the whole project. The modelling of the rotating structures is typically made with beam formulations. Many researchers adopted Euler-Bernoulli theory to investigate the vibrational behavior of spinning shafts (Bauer 1980, Chen and Liao 1991, Banerjee and Su 2004) and centrifugally stiffened beams (Banerjee 2000, Banerjee *et al*. 2006, Ozge and Kaya 2006, Mei 2008) by adopting analytical and numerical approaches to solve the equations of motion (EoM). Unfortunately, these solutions are inadequate for stubby bodies, in which rotary inertia and shear effects play an important role. To include these effects, many theories have been developed on the basis of Timoshenko beam model (Hodges and Rutkowski 1981, Curti *et al*. 1991, Curti *et al*. 1992, Rao and Gupta 2001, Banerjee 2001, Yoo *et al*. 2005). Although this formulation introduces relevant improvements, it is no longer suitable when torsion and cross-sectional warping become significant. In addition, the wide use of composite materials has introduced more difficulties in the

---

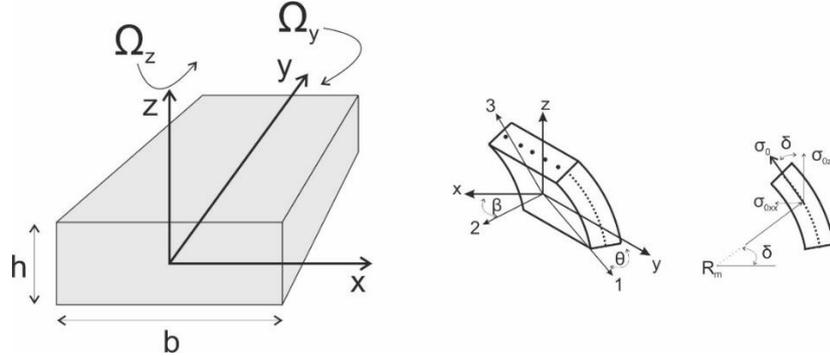∗Corresponding author, Professor, E-mail: matteo.filippi@polito.it

Fig. 1 Physical and material coordinate reference systems.

modelling of rotating structures giving a further impulse to the development of refined beam theories. For instance, advanced structural models encompassing transverse shear, secondary warping and non-uniform torsion were proposed by Song and Librescu (1997b), Chandiramani *et al*. (2002, 2003), Jung *et al*. (1999) in order to study the effects of the lamination scheme and the pretwisted angle on the rotating natural frequencies of thin-walled blade configurations. On the basis of these structural theories, critical speeds as well as stability were investigated considering spinning box beams (Song and Librescu 1997a, Song *et al*. 2000) and cylinders (Na *et al*. 2006). Jung *et al*. (2001) developed a refined 1D formulation based on a mixed variational approach to evaluate the effects of elastic coupling, shell-wall thickness, warping restraint and transverse shear deformation on the dynamics of composite rotor blades. According to this formulation, the wall was modelled as a shell while the global beam behaviour was determined using the Timoshenko theory. When the beam assumptions become too restrictive (significant cross-section deformations, elastic coupling, etc.) more sophisticated solutions are required. For instance, Genta *et al*. (1996, 2010) assumed the displacements of a thin disc as a superimposition of a rigid motion and a deflection about the rigid body configuration. According to this assumption, the last contribution was approximated with a truncated Fourier series in the tangential direction whereas, for the radial direction, polynomial functions were used. Jang and Lee (2002) used the substructure synthesis and the finite element technique for the analysis of a spinning disk-spindle system on a flexible shaft. The disc was modelled by using Kirchoff elements whereas Rayleigh and Euler-Bernoulli theories were adopted for the spindle and the stationary shaft, respectively. Furthermore, Combescure and Lazarus (2008) proposed a thorough comparison between 1D, 2D Fourier and 3D solutions for the study of the dynamics of large rotating structures. Over the years, several shell theories have been proposed to analyse the dynamics of thin (Guo *et al*. 2002, Saito and Endo 1985, Chen *et al*. 1993, Lam and Loy 1995, Ramezani and Ahmadian 2009) and thick (Guo *et al*. 2001) rotating cylindrical shells.

This paper presents an overview of the capabilities of the refined 1D models obtained through the Carrera Unified Formulation (CUF) for the study of various rotating structures. Despite being based on a 1D formulation, the present methodology provides 2D and quasi-3D results. Carrera (2002, 2003) first proposed his unified formulation for plates and shells and later for the beam approach (Carrera *et al*. 2011, Carrera *et al*. 2014a). Within the scope of this work, Carrera *et al*. (2013a, 2013b) and Carrera and Filippi (2014b, 2015) recently adopted the 1D-CUF elements to evaluate the dynamic behavior of compact isotropic and laminated shafts, rectangular composite blades and thin-walled spinning cylinders. In the following sections, further assessments are

proposed considering new rotating structures, including a membrane and laminated box beams. All results are compared with either theoretical or numerical solutions.

2. The Kinetic and potential energies

Let us consider a structure that is free to rotate about its either longitudinal or transverse axis, as shown in Fig. 1. The absolute velocity of the point P is the sum of the relative velocity and the transfer velocity

$$v_{abs} = v_{rel} + v_t = \dot{u} + \Omega \times r_{tot} \tag{1}$$

$$\Omega = \begin{bmatrix} 0 & -\Omega_z & \Omega_y \\ \Omega_z & 0 & 0 \\ -\Omega_y & 0 & 0 \end{bmatrix} \tag{2}$$

where $u = \{u_x, u_y, u_z\}^T$ is the displacement vector and $r_{tot} = r + u$ is the distance of P from the neutral axis. The kinetic energy of the whole structure is expressed by the following formula

$$T = \frac{1}{2} \int_V \rho(\dot{u}^T \dot{u} + 2\,u^T \Omega^T \dot{u} + u^T \Omega^T \Omega u + 2\dot{u}^T \Omega r + 2u^T \Omega^T \Omega r + r^T \Omega^T \Omega r) dV \tag{3}$$

In the linearized analysis, the potential energy of a rotating structure is given by the sum of the elastic term and a geometric contribution

$$U = \frac{1}{2} \int_V \left(\varepsilon_l^T C \varepsilon \right) + \left(\sigma_0 \varepsilon_{nl}^2 \right) dV \tag{4}$$

where C is the matrix of material coefficients (Carrera and Filippi 2014b) and ε_l and ε_{nl} are the linear and nonlinear components of the strain field. The term σ_0 represents the pre-stress contribution due to the rotational speed. For example, the expressions of σ_0 for a centrifugally stiffened blade ($\Omega_y = 0$) and for a spinning cylinder ($\Omega_z = 0$) are, respectively

$$\sigma_0 = \Omega_z^2 \rho \left[r_h L + \frac{1}{2} L^2 - r_h y - \frac{1}{2} y^2 \right] \tag{5}$$

$$\sigma_0 = R_m^2 \Omega_y^2 \rho \tag{6}$$

where L, r_h and R_m are the length of the beam, the dimension of the hub and the mean radius of the cylinder, respectively.

3. The Carrera unified formulation

The CUF states that the displacement field, $u(x, y, z; t)$, is an expansion of generic functions, $F_\tau(x, z)$, for the vector displacement, $u_\tau(y; t)$

$$u(x, y, z; t) = F_\tau(x, z) u_\tau(y; t), \qquad \tau = 1, 2, \ldots, T \tag{7}$$

where T stands for the number of the terms used in the expansion, and the repeated subscript, τ

indicates summation. In this work, Eq. (7) consists of Taylor-like expansions, which are functions of the coordinates of the cross-section. For example, the second-order displacement field TE2 is

$$u_x = u_{x_1} + x\,u_{x_2} + z\,u_{x_3} + x^2\,u_{x_4} + xz\,u_{x_5} + z^2\,u_{x_6}$$

$$u_x = u_{x_1} + x\,u_{x_2} + z\,u_{x_3} + x^2\,u_{x_4} + xz\,u_{x_5} + z^2\,u_{x_6}$$

$$u_x = u_{x_1} + x\,u_{x_2} + z\,u_{x_3} + x^2\,u_{x_4} + xz\,u_{x_5} + z^2\,u_{x_6}$$

The classical beam theories are obtainable as particular cases of the linear expansion, TE1. It should be noted that classical theories require reduced material stiffness coefficients to contrast Poisson's locking. Unless otherwise specified, for classical and first-order models Poisson's locking is corrected according to (Carrera *et al.* 2014a). According to the Finite Element technique, the generalized displacement vector becomes

$$\boldsymbol{u}_\tau(y; t) = N_i(y)\boldsymbol{q}_{\tau i}(t) \tag{8}$$

where $N_i(y)$ are the shape functions and $\boldsymbol{q}_{\tau i}(t)$ is the nodal displacement vector $\boldsymbol{q}_{\tau i}(t) = \left\{ q_{u_{x\tau i}}, q_{u_{y\tau i}}, q_{u_{z\tau i}} \right\}^{\mathrm{T}}$.

4. Governing equations of rotating and spinning structures

The EoM are obtained through the Hamilton's Principle

$$\delta \int_{t0}^{t1} (T - U)dt = 0 \tag{9}$$

in which δ is the virtual variation of the functional. The homogeneous EoM are

$$\boldsymbol{M}\ddot{q} + \boldsymbol{G}_\Omega \dot{q} + \left(\boldsymbol{K} + \boldsymbol{K}_\Omega + \boldsymbol{K}_{\sigma_0} \right) = 0 \tag{10}$$

where the matrices are written in terms of '*fundamental nuclei*'. Besides the mass and stiffness matrices, $\boldsymbol{M}^{ij\tau s}$ and $\boldsymbol{K}^{ij\tau s}$, the other three contributions are: the Coriolis matrix $\boldsymbol{G}^{ij\tau s}$, the softening matrix $\boldsymbol{K}_\Omega^{ij\tau s}$ and the centrifugal stiffening matrix $\boldsymbol{K}_{\sigma_0}^{ij\tau s}$ due to the rotation.

$$\boldsymbol{M}^{ij\tau s} = I_l^{ij} \lhd (F_\tau \rho I F_s) \rhd$$

$$\boldsymbol{G}^{ij\tau s} = 2\boldsymbol{\Omega}\, I_l^{ij} \lhd (F_\tau \rho I F_s) \rhd$$

$$\boldsymbol{K}_\Omega^{ij\tau s} = \boldsymbol{\Omega}^T \boldsymbol{\Omega}\, I_l^{ij} \lhd (F_\tau \rho I F_s) \rhd$$

$$\boldsymbol{K}^{ij\tau s} = I_l^{ij} \lhd \boldsymbol{D}_{np}^T (F_\tau I) \big[\boldsymbol{C}_{np} \boldsymbol{D}_p (F_s I) + \boldsymbol{C}_{nn} \boldsymbol{D}_{np}(F_s I) \big] +$$

$$+\boldsymbol{D}_p^T (F_\tau I) \big[\boldsymbol{C}_{pp} \boldsymbol{D}_p (F_s I) + \boldsymbol{C}_{pn} \boldsymbol{D}_{np}(F_s I) \big] \rhd$$

$$+ I_l^{ij,y} \lhd [\boldsymbol{D}_{np}^T (F_\tau I) + \boldsymbol{D}_p^T (F_\tau I)\, \boldsymbol{C}_{pn}]\, F_s \rhd I_{Ay}$$

$$+ I_l^{i,yj} I_{Ay}^T \lhd F_\tau\, [\boldsymbol{C}_{np} \boldsymbol{D}_p^T (F_s I) + \boldsymbol{C}_{nn} \boldsymbol{D}_{np}^T(F_s I)] \rhd$$

$$+ I_l^{i,yj,y} I_{Ay}^T I_{Ay} \lhd F_\tau \boldsymbol{C}_{nn} F_s \tag{11a}$$

The expressions of the centrifugal stiffening fundamental nuclei for a spinning and rotating structure are, respectively

$$\boldsymbol{K}_{\sigma_0}^{ij\tau s} = I_l^{ij} \lhd \left(F_{\tau,x} \sigma_{0_{xx}} \boldsymbol{I} F_{s,x} \right) + \left(F_{\tau,z} \sigma_{0_{zz}} \boldsymbol{I} F_{s,z} \right) + \left(F_{\tau,x} \sigma_{0_{xz}} \boldsymbol{I} F_{s,z} \right) + \left(F_{\tau,z} \sigma_{0_{zx}} \boldsymbol{I} F_{s,x} \right) \rhd$$

$$\boldsymbol{K}_{\sigma_0}^{ij\tau s} = I_{l\sigma_0}^{i,yj,y} \boldsymbol{\Omega}^T \boldsymbol{\Omega} \lhd (F_\tau \rho \boldsymbol{I} F_s) \rhd \tag{11a}$$

where

$$\boldsymbol{I}_{Ay} = \begin{bmatrix} 0 & 0 & 1 \\ 1 & 0 & 0 \\ 0 & 1 & 0 \end{bmatrix} \; ; \; \boldsymbol{I} = \begin{bmatrix} 1 & 0 & 0 \\ 0 & 1 & 0 \\ 0 & 0 & 1 \end{bmatrix}$$

$$\lhd \cdots \rhd = \int_A \ldots dA$$

$$I_l^{ij}, I_l^{ij,y}, I_l^{i,yj}, I_l^{i,yj,y}, I_{l\sigma_0}^{i,yj,y} = \int_l (N_i N_j, \; N_i N_{j,y}, N_{i,y} N_j, N_{i,y} N_{j,y}, \sigma_0 N_{i,y} N_{j,y}) \, dy$$

The terms $\sigma_{0_{xx}}, \sigma_{0_{zz}}, \sigma_{0_{xz}}$ are the components of the pre-stress distribution of Eq. (6) written in the Cartesian coordinate system.

5. Numerical results

5.1 Spinning structures

5.1.1 Thin-walled cylinder

A clamped-clamped cylinder with the wall thickness, $t=0.05$ m, mean diameter, $d=1.0$ m, and length, $L=3$ m, is considered. The Young's modulus, Poisson's ratio and density are $E=207$ Gpa, $v=0.3$ and $\rho=7860$ kg/m^3, respectively. The mathematical model consists of seven 4-node beam elements along the longitudinal direction. With purposes of comparison, the natural frequencies in the non-rotating state are compared in Table 1 with those obtained with a 2D Nastran finite element solution. The first two columns report the wave numbers along the circumferential and longitudinal directions, respectively. The comparisons reveal that the TE8 theory predicts

Table 1 Natural frequencies [Hz] of the non-rotating cylinder

n	m	TE7	TE8	2D Nastran
2	1	223.77	223.62	222.08
1	1	336.88	336.88	335.26
3	1	472.64	400.72	394.78
2	2	417.48	417.06	414.59
3	2	547.10	484.49	473.00
Torsional		530.44	530.44	527.69
3	3	679.18	627.69	609.04
2	3	652.89	652.11	647.17
1	2	664.21	664.21	661.02

Table 2 Dimensionless frequencies for various rotational speed values.

N	Ω/f_n		Eq. (12)	Eq. (13)	Eq. (14)	TE8
2	0.1	forward	0.9262	0.9272	0.9351	0.9276
		backward	1.0862	1.0872	1.0951	1.0870
	0.2	forward	0.8645	0.8684	0.8991	0.8696
		backward	1.1845	1.1884	1.2191	1.1879
	0.3	forward	0.8143	0.8228	0.8885	0.8245
		backward	1.2943	1.3028	1.3685	1.3019
	0.4	forward	0.7747	0.7892	0.8992	0.7910
		backward	1.4147	1.4292	1.5392	1.4282
	0.5	forward	0.7446	0.7662	0.9266	0.7678
		backward	1.5446	1.5662	1.7266	1.5647
3	0.1	forward	0.9679	0.9684	0.9771	0.9688
		backward	1.0879	1.0884	1.0971	1.0883
	0.2	forward	0.9874	0.9892	1.0212	0.9894
		backward	1.2274	1.2292	1.2612	1.2286
	0.3	forward	1.0486	1.0522	1.1163	1.0517
		backward	1.4086	1.4122	1.4763	1.4111
	0.4	forward	1.1404	1.1462	1.2465	1.1436
		backward	1.6204	1.6262	1.7265	1.6248
	0.5	forward	1.2540	1.2620	1.4000	1.2559
		backward	1.8540	1.8620	2.000	1.8602

frequencies and mode shapes with significant accuracy, while the TE7 overestimates the frequencies relating to the mode shapes with n=3.

To evaluate the effects of the rotational speed on the dynamic behavior, Table 2 lists the non-dimensional backward and forward frequencies computed with the TE8 theory for the mode shapes with n=2, 3 and m=1. The 1D-CUF results are compared with the following analytical solutions based on based on the following shell formulations (Chen *et al.* 1993)

$$\frac{f}{f_n} = \frac{2n}{n^2+1}\left(\frac{\Omega}{f_n}\right) \pm \sqrt{1 + \frac{n^6 - 2n^4 - 1}{(n^2+1)^2}\left(\frac{\Omega}{f_n}\right)^2} \tag{12}$$

$$\frac{f}{f_n} = \frac{2n}{n^2+1}\left(\frac{\Omega}{f_n}\right) \pm \sqrt{1 + \frac{n^2(n^2-1)^2}{(n^2+1)^2}\left(\frac{\Omega}{f_n}\right)^2} \tag{13}$$

$$\frac{f}{f_n} = \frac{2n}{n^2+1}\left(\frac{\Omega}{f_n}\right) \pm \sqrt{1 + \frac{n^6 + 3n^2}{(n^2+1)^2}\left(\frac{\Omega}{f_n}\right)^2} \tag{14}$$

where f_n is the natural frequency at $\Omega = 0$. It is observed that the 1D-CUF results strongly agree with those predicted by Eqs. (12)-(13) while, in contrast, discrepancies are evident with respect to

the solution of Eq. (14). As pointed out in (Chen *et al*. 1993), the differences arise from the differing treatments of high order infinitesimal various shell theories.

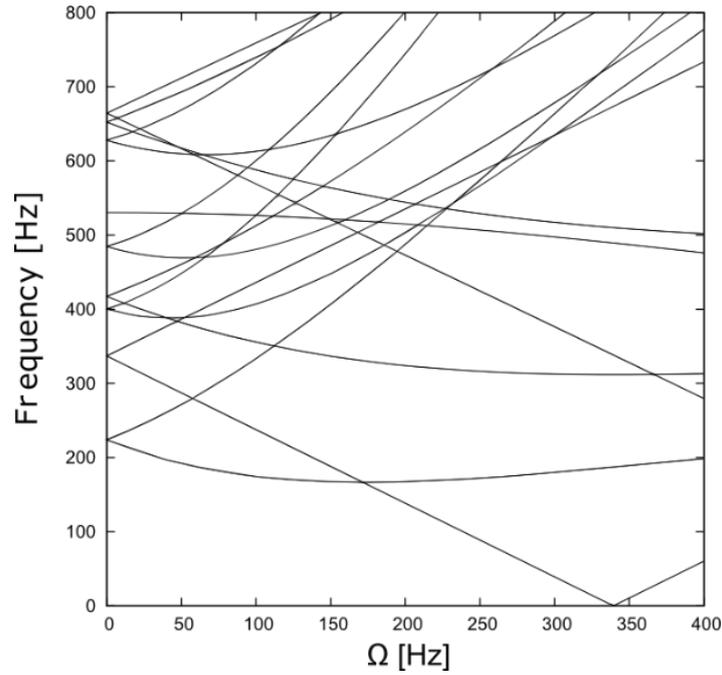Fig. 2 graphically shows the frequency variations related to the mode shapes of Table 1.

Fig. 1 Frequency vs. angular speed of the clamped-clamped cylinder

5.1.2 Thin membrane

In the second numerical application, a circular membrane with the thickness, t=0.002 m and outer diameter, d_o=1.05 m, is considered. The mathematical model consists of two 4-node beam elements along the longitudinal direction, and the structure is not constrained. The frequencies in the non-rotating state computed with the TE8 expansion are compared with those obtained through a Nastran 2D solution in order to evaluate the accuracy of the proposed methodology (see Table 3).

It should be noted that the 1D-CUF elements ensure a significant accuracy in the prediction of frequencies and mode shapes. The highest relative difference between the two finite element solutions is about 4.5%. According to Southwell's theory, the natural frequencies of a rotating membrane with the bending stiffness vanishingly small are proportional to the spin speed, i.e.,

$$\omega = \beta\Omega \tag{15}$$

where β is a coefficient depending on the numbers of nodal diameters, 'm', and nodal circles, 'n', coming from the following expression

$$\beta_i = \sqrt{\frac{3+\nu}{8}(m+2n)(m+2n+2) - m^2\frac{1+3\nu}{8}}$$

Table 3 Natural frequencies [Hz] of the non-rotating membrane

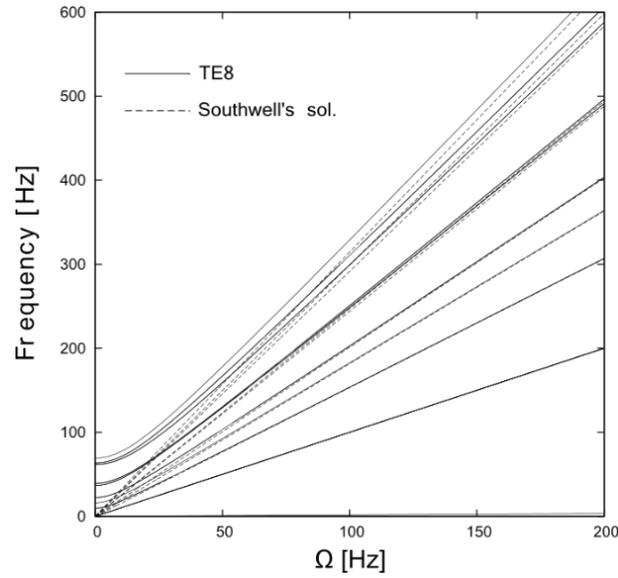| Mode shape	TE8	2D Nastran	% diff.	β
	Rigid motion	Rigid motion	-	1.0000
	9.611	9.542	0.723	1.5330
	16.15	16.01	0.874	1.8166
	22.31	22.04	1.225	2.0125
	36.75	36.02	2.026	2.4393
	39.18	38.55	1.634	2.4698
	61.45	58.80	4.506	2.9155
	63.38	61.73	2.673	2.9917
	69.25	67.90	1.988	3.1464

Fig. 1 Frequency vs. angular speed of the thin membrane

The β values for the considered mode shapes are reported in the last column of Table 3. For this structure, the circumferential and radial pre-stress distribution are

$$\sigma_{\delta\delta} = \rho\Omega^2 \frac{(3-2\nu)}{8(1-\nu)}[r_0^2 + r_i^2 - \frac{r_0^2 r_i^2}{r^2} - r^2]$$

$$\sigma_{rr} = \rho\Omega^2 \frac{(3-2\nu)}{8(1-\nu)}[r_0^2 + r_i^2 + \frac{r_0^2 r_i^2}{r^2} - \frac{(1+2\nu)}{(3-2\nu)}r^2]$$

where 'r_i', 'r_0' are the inner and outer radii. The frequency curves are shown in Fig. 2. It should be noted that the frequency branches predicted with the present formulation asymptotically follow the curves of Eq. (15) for relatively high speeds when the centrifugal stiffness supplies the in-plane stretching.

5.2 Rotating blades

5.2.1 Laminated beams

The structures are two graphite-epoxy rectangular beams whose width is c=25.4 mm. The thickness and fiber orientations are different for the two cases, and they are listed in Table 4 with the relating material properties. The beam length, L, is a problem parameter and, two different aspect ratios are studied (L/c=10, 20). The cantilevered blade configurations are modelled using eight 4-node beam elements. The reference solutions are taken from (Yeo *et al.* 2010), where the authors presented comparisons between 1D and 3D formulations for various blade configurations. In particular, the 1D beam analyses were performed using the Variational Asymptotic Beam Sectional (VABS) approach in order to compute the 2D cross-sectional properties of the blade, whereas the 3D solutions were obtained with the commercial code MSC/Marc.

Table 4 Material properties and thicknesses of the graphite-epoxy laminated beams

Case	Thickness [mm]	Fiber Orientation [deg]
1	2.97	0°
2	3.22	15°
Property		
E_{11}	142.0 [GPa]	
$E_{22}=E_{33}$	9.80 [GPa]	
$G_{21}=G_{31}$	6.00 [GPa]	
G_{32}	6.00 [GPa]	
$v_{12}=v_{13}$	0.42	
v_{23}	0.54	
ρ	1538 [kg/m^3]	

Fig. 3 shows the frequency variations for the [0°] lamination sequence obtained with various TE models. For L/c=20, it is observed that all theories provide almost the same results except for slight difference in the computation of the second torsional frequency curve. When the L/c ratio decreases, the 1D-VABS solution underestimates the second and third torsional frequencies with respect to TE and 3D models. Moreover, it should be noted that the increasing of the TE order ensures the convergence of the proposed results to the solid solution. Regarding the [15°] lamination sequence, the results are shown in Fig. 4. Due to the bending-torsion coupling, the discrepancies between the 1D-VABS and the other theories (TE and 3D) are also evident for the third, fourth and fifth flapping modes. Despite the significant coupling effects, the TE elements provide results very close to solid solutions for both considered L/c ratios.
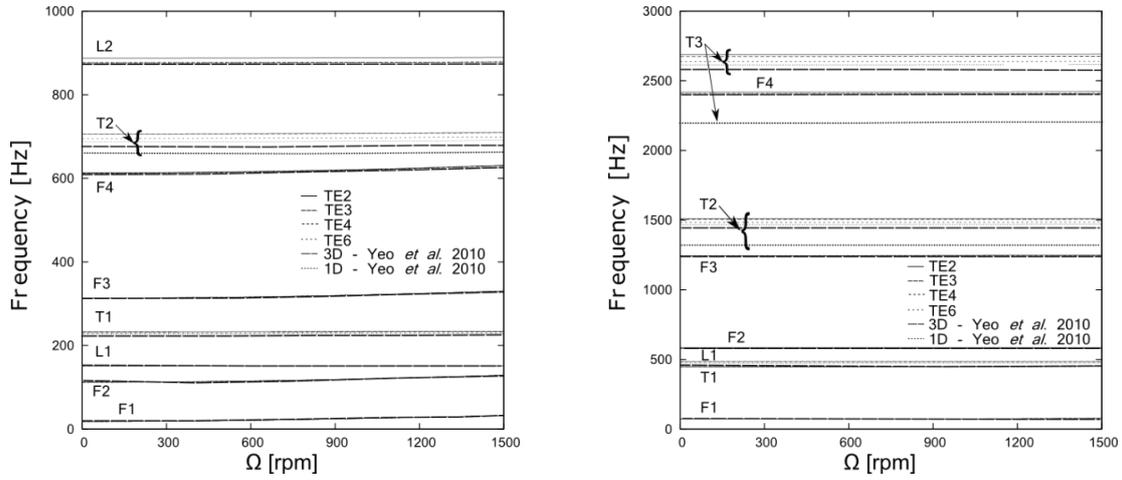
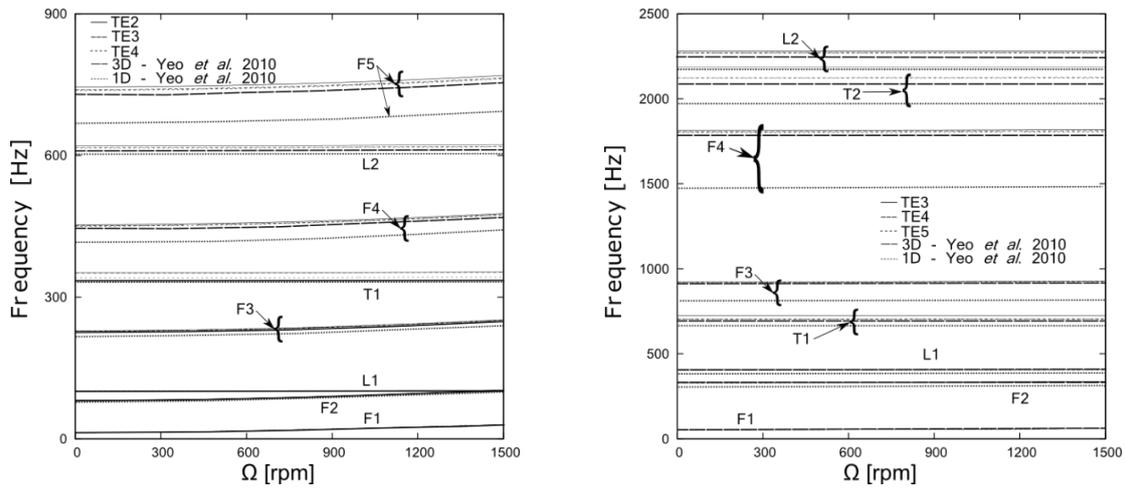Fig. 3 Frequency comparison for graphite-epoxy beam, [0°]. *L/c*=20 (left) and 10 (right)

Fig. 4 Frequency comparison for graphite-epoxy beam, [15°]. *L/c*=20 (left) and 10 (right)

5.2.2 Thin-walled box beams

The structures are three thin-walled box beams previously analysed in Chandra *et al*. (1992). The length of structures is *L*=0.8446 m while the wall thicknesses and material properties are different for the three cases. For the sake of completeness, the problem parameters are reported in Table 5. For the first two structures, each edge is constituted by two orthotropic layers according to the following stacking sequence: top and bottom flanges [45°/45°] and right and left webs [45°/-45°]. For the third beam configuration, all edges are made of six layers with the $[15°]_6$ lamination scheme. The cantilevered structures are modelled using ten 4-node beam elements.

For the first two cases, the analyses have been performed with three different Taylor-like expansions, namely the TE2, TE3 and TE4. The results are shown in Fig. 5, where they are compared with theoretical and experimental data provided in Chandra *et al*. (1992). In particular, for the Kevlar-epoxy beam, it is observed that TE2 and TE3 expansions provide almost the same results. On the other hand, adopting the TE4 theory, the second flapping frequency decreases

Table 5 Material and geometrical properties of the box beams

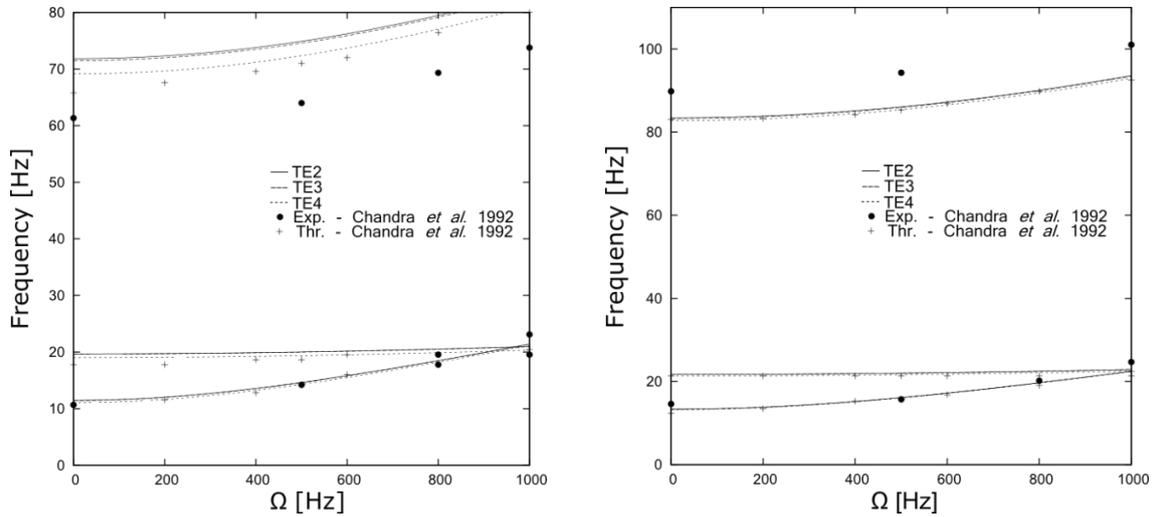|	Case 1	Case 2	Case 3
Ply thickness (mm)	0.254	0.4064	0.127
Inner dimensions (mm)	22.6822×0.0121158	22.6822×0.0121158	22.6822×0.0121158
Material properties	Kevlar-epoxy	Glass-epoxy	Graphite-epoxy
E_{11} (GPa)	75.84	48.26	141.9
$E_{22}=E_{33}$ (GPa)	5.52	14.48	9.78
$G_{21}=G_{31}$ (GPa)	2.34	5.52	6.13
$v_{12}=v_{13}$	0.34	0.26	0.42
ρ (kg/m^3)	1113.1	1790.3	1449.0

Fig. 5 Natural frequencies of box beams: Kevlar-epoxy (left) and glass-epoxy (right)

Table 6 Rotating natural frequencies [Hz] of the $[15°]_6$ box beam

Mode	Exp. (Chandra *et al.* 1992)	Thr. (Chandra *et al.* 1992)	Thr. (Stemple *et al.* 1989)	Thr. (Smith *et al.* 1991)	Thr. (Jung *et al.* 2001)	Present TE4	Present TE5
Flap 1	35.2	35.4	36.00	36.87	35.58	35.86	35.02
Lag 1	46.6	45.9	47.31	53.73	45.45	51.13	48.44
Flap 2	184.0	185.0	188.0	202.2	182.1	196.4	190.5
Lag 2	N/A	N/A	287.2	328.2	277.5	312.9	296.9
Torsion 1	N/A	N/A	513.2	493.7	495.5	527.3	527.8

getting close to the reference theoretical prediction. Moreover, for the second flapping mode, all theoretical results are higher than the experimental data with a correlation within 10%. Regarding the second case (glass-epoxy beam), TE expansions strongly agree with the reference theoretical results. All theories predict lower frequency values for the second flapping mode shape with respect to the experimental data.

The rotating frequencies (at Ω=1002 rpm) of the third configuration are reported in Table 6. They are compared with experimental and theoretical values found in Jung *et al*. (2001). In particular, the theoretical results were obtained through various advanced one-dimensional formulations, which included shear and warping deformability. It is observed that the 1D-CUF models provide results close to the reference solutions, except for a slight difference in the computation of the torsional frequency. Furthermore, the increasing of the theory order yields a decreasing of the frequency values until to 5%.

6. Conclusions

In the present paper, the Carrera Unified Formulation has been extended to the free vibration of rotating and spinning structures. The equations of motion were derived through Hamilton's Principle and solved with the Finite Element Method. Metallic and composite rotating beams were considered and, to assess the new theory, the results were compared with those published in the literature, when possible. The hierarchical property of CUF enables one to obtain refined displacement fields. The equations are written in a fully three-dimensional form and, in the light of the results, it is possible to make the following remarks:
   • the proposed approach represents a tool for the study of many rotating structures including blade configurations and thin-walled structures made of metallic and composite materials;
   • the refined beam theories enables one to predict to predict shell-like mode shapes and frequencies of thin-walled structures with significant accuracy;
   • the formulation includes the press-stress also for the spinning structures;
   • the 1D-CUF elements perfectly reproduce the solid solutions also when structural couplings due to the lamination sequence occur.
In conclusion, the 1D-CUF theory appears very attractive for the study of rotordynamics since it ensures accurate results with a low computational effort. Despite being a beam formulation, it allows to include the initial in-plane stresses. In this way, the main drawbacks of the classical beam and shell theories can be easily overcome considering, with the same theoretical approach, thick and thin cylinders, deformable disks and laminated blades. Future work could be devoted, therefore, to the study of more complex spinning structures (conical shells, multi-sections shaft, etc.) and the effects of longitudinal and transverse stiffeners.

References

Banerjee, J. (2000), "Free vibration of centrifugally stiffened uniformand tapered beams using the dynamic stiffness method", *J. Sound Vib.*, **233**, 857-875.
Banerjee, J. (2001), "Dynamic stiffness formulation and free vibration analysis of centrifugally stiffened Timoshenko beams", *J. Sound Vib.*, **247**, 97-115.
Banerjee, J. and Su, H. (2004), "Development of a dynamic stiffness matrix for free vibration analysis of spinning beams", *Comput. Struct.*, **82**, 2189-2197.
Banerjee, J., Su, H. and Jackson, D. (2006), "Free vibration of rotating tapered beams using the dynamic stiffness method", *J. Sound Vib.*, **298**, 1034-1054.
Bauer, H. (1980), "Vibration of a rotating uniform beam, part 1: Orientation in the axis of rotation", *J. Sound Vib.*, **72**, 177-189.
Carrera, E. (2002), "Theories and finite elements for multilayered, anisotropic, composite plates and shells",

Arch. Comput. Meth. Eng., **9**(2), 87-140.

Carrera, E. (2003), "Theories and finite elements for multilayered plates and shells: a unified compact formulation with numerical assessment and benchmarking", *Arch. Comput. Meth. Eng.*, **10**(3), 215-296.

Carrera, E., Giunta, G. and Petrolo, M. (2011), *Beam Structures, Classical and Advanced Theories,* Wiley.

Carrera, E., Cinefra, M., Petrolo, M. and Zappino, E. (2014a), *Finite Element analysis of structures through Unified Formulation,* Wiley.

Carrera, E., Filippi, M. and Zappino, E. (2013a), "Analysis of rotor dynamic by one-dimensional variable kinematic theories", *J. Eng. Gas Turb. Power*, **135**, 092501.

Carrera, E., Filippi, M. and Zappino, E. (2013b), "Free vibration analysis of rotating composite blades via carrera unified formulation", *Compos. Struct.*, **106**, 317-325.

Carrera, E. and Filippi, M. (2014b), "Variable kinematic one-dimensional finite elements for the analysis of rotors made of composite materials", *J. Eng. Gas Turb. Power*, **136**, 092501.

Carrera, E. and Filippi, M. (2015), "Vibration analysis of thin/thick, composites/metallic spinning cylindrical shells by refined beam models", *J. Vib. Acoust.*, ASME, **137**(3), 031020.

Chandiramani, N., Librescu, L. and Shete, C. (2002), "On the free-vibration of rotating composite beams using a higher-order shear formulation", *Aerosp. Sci. Tech.*, **6**, 545-561.

Chandiramani, N., Librescu, L. and Shete, C. (2003), "Vibration of higher-order-shearable pretwisted rotating composite blades", *Int. J. Mech. Sci.*, **45**, 2017-2041.

Chandra, R. and Chopra, I. (1992), "Experimental-theoretical investigation of the vibration characteristics of rotating composite box beams", *J. Aircraf.*, **29**, 657-664.

Chen, M. and Liao, Y. (1991), "Vibrations of pretwisted spinning beams under axial compressive loads with elastic constraints", *J. Sound Vib.*, **147**, 497-513.

Chen, Y., Zhao, H., Shen, Z., Grieger, I. and Kroplin, B.H. (1993), "Vibrations of high speed rotating shells with calculations for cylindrical shells", *J. Sound Vib.*, **160**, 137-160.

Combescure, D. and Lazarus, A. (2008), "Refined finite element modelling for the vibration analysis of large rotating machines: application to the gas turbine modular helium reactor power conversion unit", *J. Sound Vib.*, **318**(4), 1262-1280.

Curti, G., Raffa, F. and Vatta, F. (1991), "The dynamic stiffness matrix method in the analysis of rotating systems", *Tribol. Tran.*, **34**, 81-85.

Curti, G., Raffa, F. and Vatta, F. (1992), "An analytical approach to the dynamics of rotating shafts", *Meccanica*, **27**, 285-292.

Genta, G., Chen, F. and Tonoli, A. (2010), "Dynamics behavior of rotating bladed discs: a finite element formulation for the study of second and higher order harmonics", *J. Sound Vib.*, **329**, 5289-5306.

Genta, G. and Tonoli, A. (1996), "A harmonic finite element for the analysis of flexural, torsional and axial rotordynamics behavior of discs", *J. Sound Vib.*, **196**, 19-43.

Guo, D., Chu, F. and Zheng, Z. (2001), "The influence of rotation on vibration of a thick cylindrical shell", *J. Sound Vib.*, **242**, 487-505.

Guo, D., Zheng, Z. and Chu, F. (2002), "Vibration analysis of spinning cylindrical shells by finite element method", *Int. J. Solid. Struct.*, **39**, 725-739.

Hodges, D. and Rutkowski, M. (1981), "Free-vibration analysis of rotating beams by a variable-order finite-element method", *AIAA J.*, **19**, 1459-1466.

Jang, G.H., Lee, S.H. and Jung, M.S. (2002), "Free vibration analysis of a spinning flexible disk-spindle system supported by ball bearing and flexible shaft using the finite element method and substructure synthesis", *J. Sound Vib.*, **251**, 59-78.

Jung, S.N., Nagaraj, V. and Chopra, I. (1999), "Assessment of composite rotor blade modeling techniques", *J. Am. Helicop. Soc.*, **44**, 188-205.

Jung, S.N., Nagaraj, V. and Chopra, I. (2001), "Refined structural dynamics model for composite rotor blades", *AIAA J.*, **39**, 339-348

Lam, K.Y. and Loy, C.T. (1995), "Free vibrations of a rotating multilayered cylindrical shell", *Int. J. Solid. Struct.*, **32**, 647-663.

Mei, C. (2008), "Application of differential transformation technique to free vibration analysis of a

centrifugally stiffened beam", *Comput. Struct*., **86**, 1280-1284.

Na, S., Yoon, H. and Librescu, L. (2006), "Effect of taper ratio on vibration and stability of a composite thin-walled spinning shaft", *Thin Wall. Struct.*, **44**, 362-371.

Ozge, O.O. and Kaya, M.O. (2006), "Flapwise bending vibration analysis of double tapered rotating Euler-Bernoulli beam by using the differential transform method", *Meccanica*, **41**, 661-670.

Ramezani, S. and Ahmadian, M. (2009), "Free vibration analysis of rotating laminated cylindrical shells under different boundary conditions using a combination of the layer-wise theory and wave propagation approach", *Tran. B: Mech. Eng.*, **16**, 168-176.

Rao, S. and Gupta, R. (2001), "Finite element vibration analysis of rotating Timoshenko beams", *J. Sound Vib.*, **242**, 103-124.

Saito, T. and Endo, M. (1985), "Vibration of finite length rotating cylindrical shells", *J. Sound Vib.*, **107**, 17-28.

Song, O. and Librescu, L. (1997a), "Anisotropy and structural coupling on vibration and instability of spinning thin-walled beams", *J. Sound Vib.*, **204**, 477-494.

Song, O. and Librescu, L. (1997b), "Structural modeling and free vibration analysis of rotating composite thin-walled beams", *J. Am. Helicop. Soc.*, **42**, 358-369.

Song, O., Librescu, L. and Jeong, N.H. (2000), "Vibration and stability of prestwisted spinning thin-walled composite beams featuring bending-bending elastic coupling", *J. Sound Vib.*, **237**, 513-533.

Yeo, H., Truong, K.V. and Ormiston, R.A. (2010), "Assessment of 1-D Versus 3-D Methods for Modeling Rotor Blade Structural Dynamics", *51st AIAA/ASME/ASCE/AHS/ASC Structures, Structural Dynamics, and Materials Conference,* Orlando, April.

Yoo, H.H., Lee, S.H. and Shin, S.H. (2005), "Flapwise bending vibration analysis of rotating multilayered composite beams", *J. Sound Vib.*, **286**, 745-761.